Supplementary Material

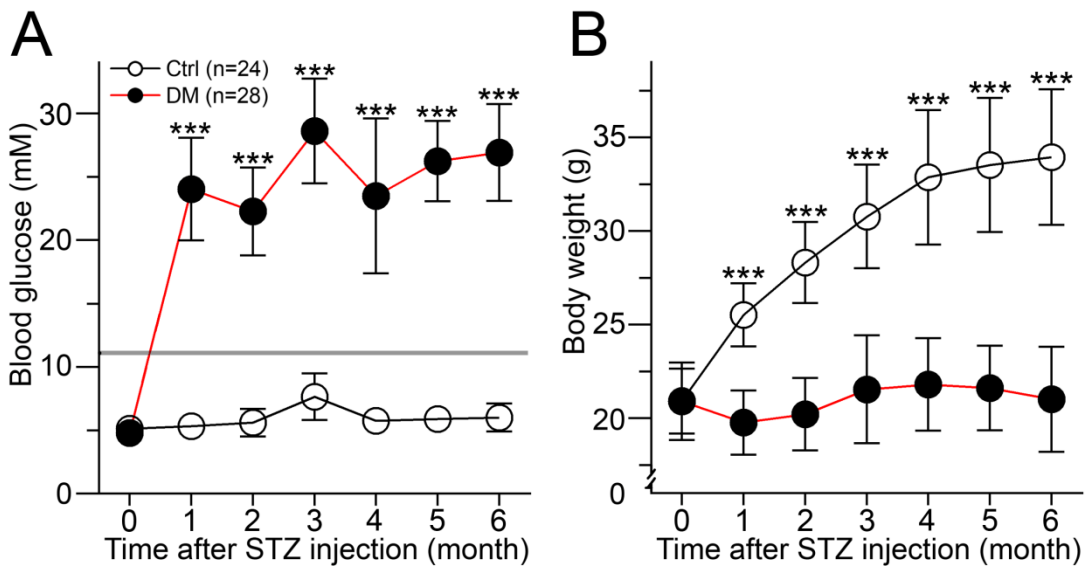

Supplementary Figure 1. Diabetes caused significant changes in blood glucose levels and body weight. (**A**) Blood glucose levels of control and DM C57BL/6 mice as a function of time. After DM induction, blood glucose levels in the STZ-treated mice were increased by over 3-fold as compared with control animals over the course of six months. The grey line indicates the blood glucose level of 11.1 mM. (**B**) Growth curves of control and DM mice. Control mice gained weight continuously; in contrast, DM mice showed very limited weight increase over six months. Sample sizes are given in parentheses. ***$P < 0.001$.

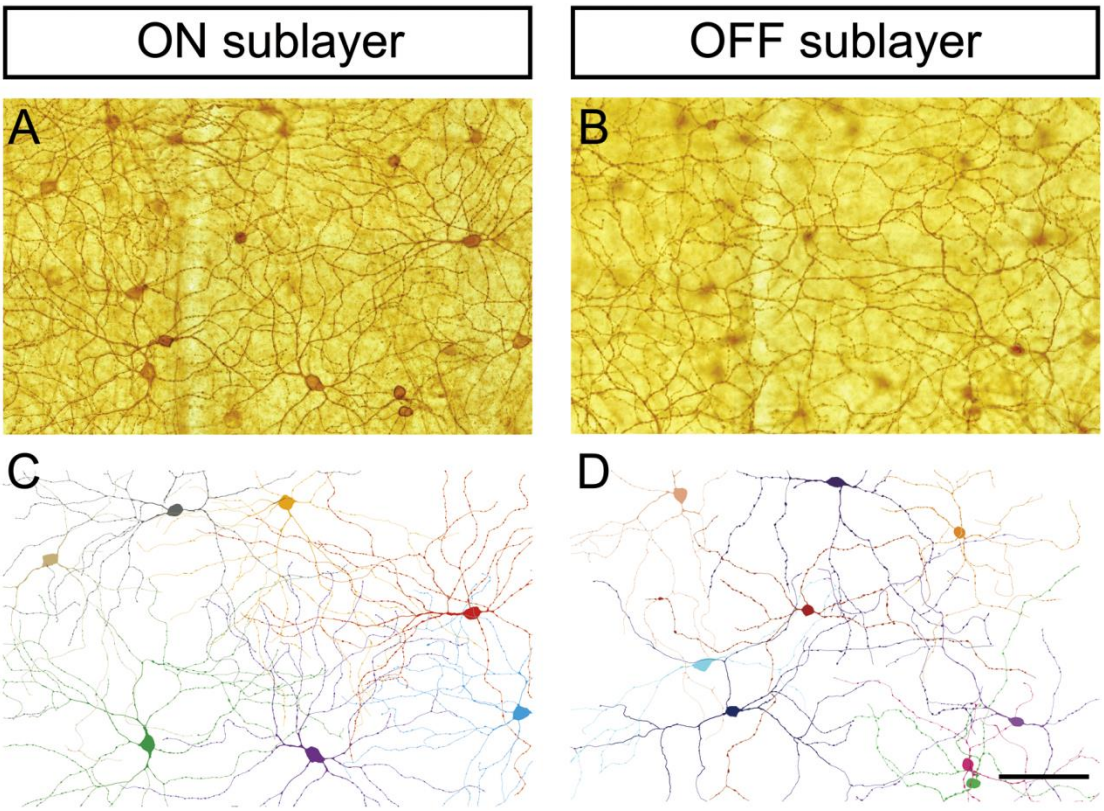

Supplementary Figure 2. Melanopsin-positive plexuses in the inner and outer sublaminae of the IPL revealed by the UF006 antibody. (**A, B**) Two representative photomicrographs of a retinal region in a whole-mount preparation stained with UF006 melanopsin antibody using immunoperoxidase method. The focal plane of (**A**) lies in the inner part of the IPL, where the dendritic networks of M2 ipRGCs reside in, and that of (**B**) lies in the outermost level of the IPL, where the M1 plexuses are located. (**C, D**) Reconstruction of the mosaic comprising of M2 (**C**) and M1 (**D**) cells in the area shown in (**A**) and (**B**). Scale bar = 100 μm.

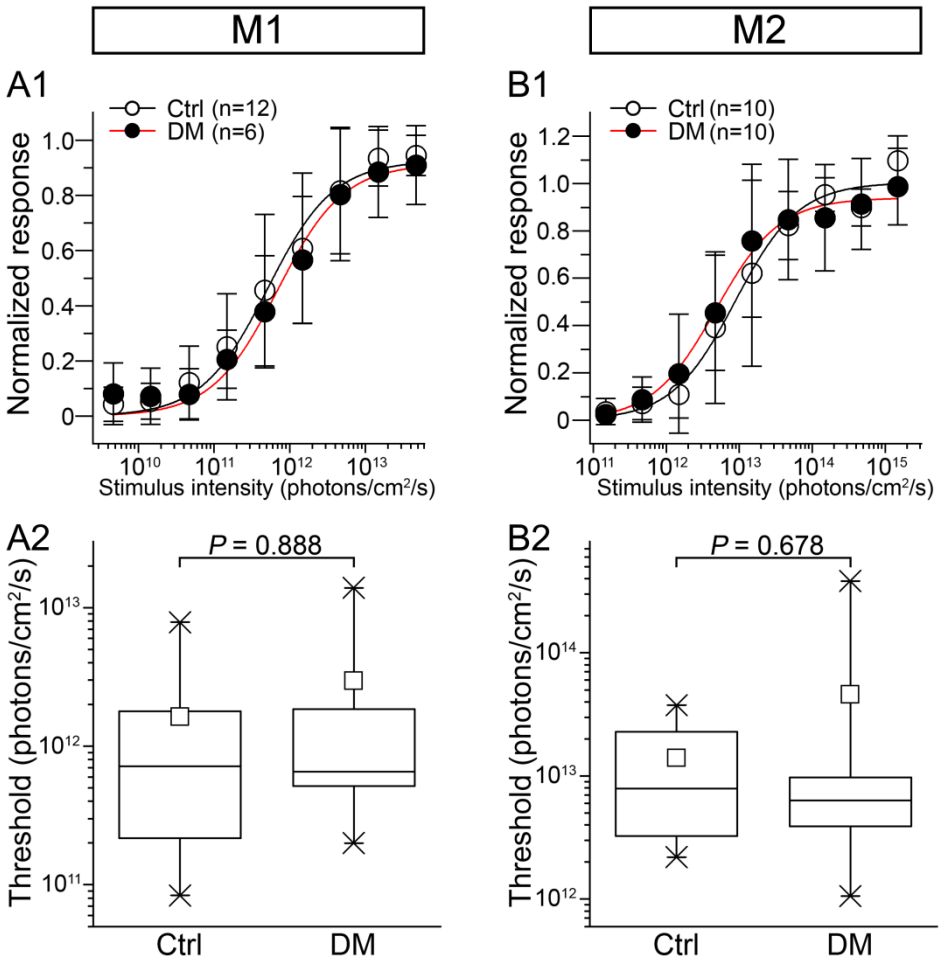

Supplementary Figure 3. Diabetes did not change response thresholds of M1 or M2 ipRGCs. (**A1, B1**) Michaelis–Menten equation-fitted I–R curves based on peak depolarization data obtained using patch-clamp recording in M1 (**A1**) and M2 (**B1**) cells. (**A2, B2**) Box plots showing no significant difference in photoresponse threshold between control and DM retinas for either M1 (**A2**) or M2 (**B2**) cells. Sample sizes are given in parentheses.

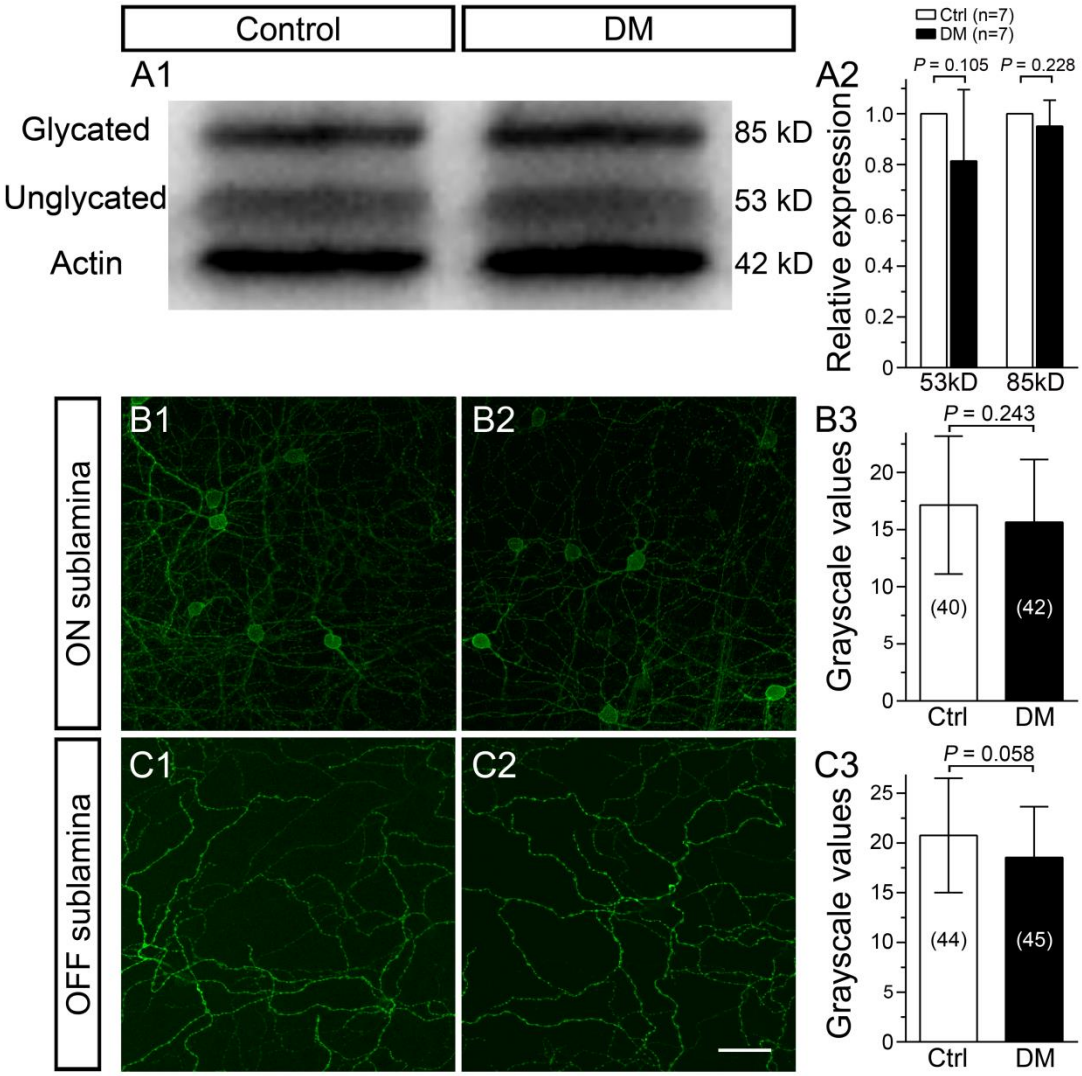

Supplementary Figure 4. Diabetes did not alter melanopsin protein expression levels. (**A1**) Representative photograph of Western blot of whole retina homogenates in control and DM mice for the PA1-780 melanopsin antibody. (**A2**) Densitometric analysis revealed that whole-retina melanopsin proteins levels were unchanged in DM mice. (**B1, B2, C1, C2**) Representative fluorescence photomicrographs of whole-mount retinas stained with UF006 melanopsin antibody from control (**B1, C1**) and DM (**B2, C2**) mice, showing melanopsin-positive plexuses in the ON (**B1, B2**; mainly composed of M2 dendrites) and OFF (**C1, C2**; mainly composed of M1

dendrites) sublamina of the IPL . (**B3, C3**) In both sublaminae, control and DM mice showed similar fluorescence intensities of melanopsin-positive processes, quantified by measuring mean gray levels within the area occupied by melanopsin-positive processes. Scale bar = 100 μm. Sample sizes are given in parentheses.

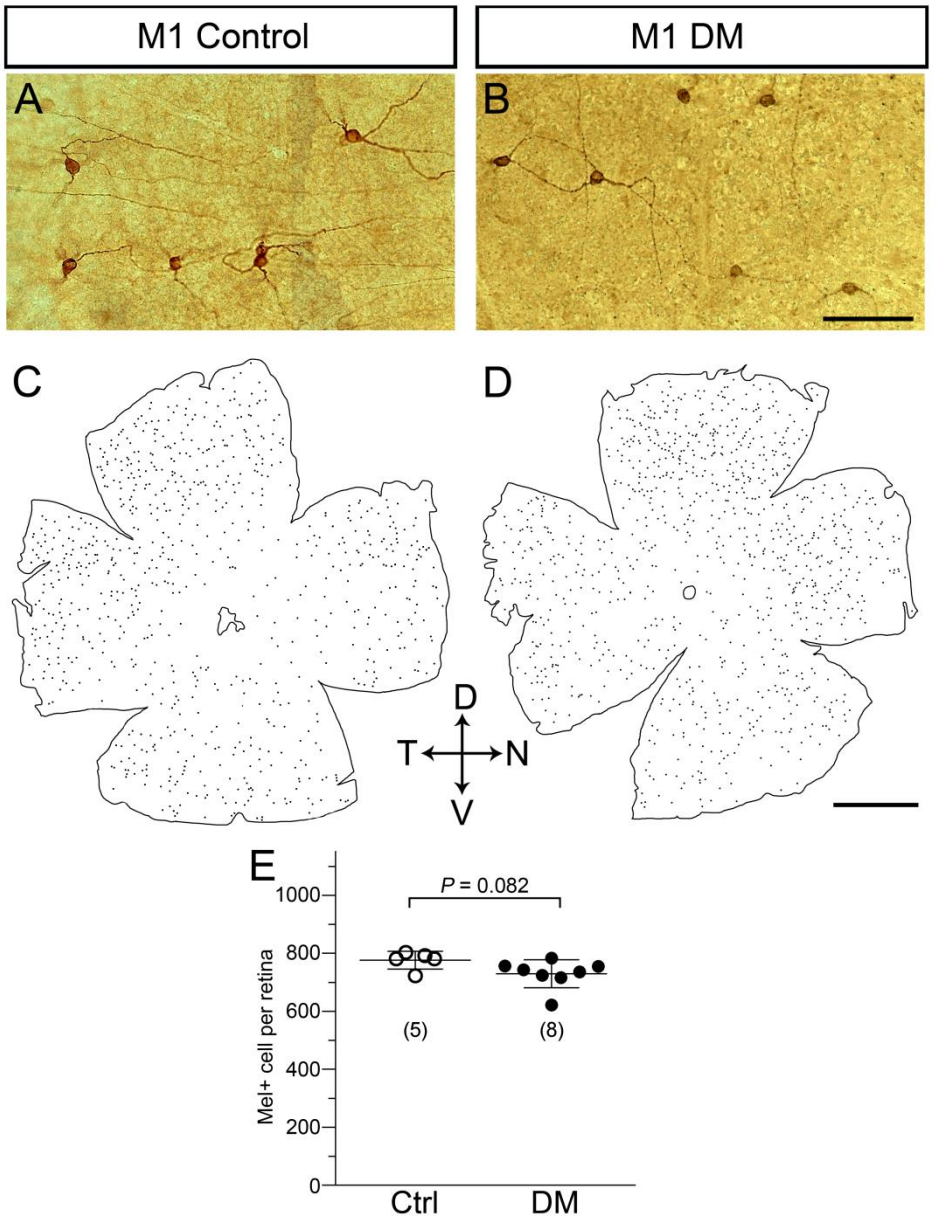

Supplementary Figure 5. No significant loss of M1 ipRGCs in 6-month diabetic mice. (**A, B**) Representative photomicrographs, captured from a small area within whole-mount retinas stained by enhanced immunohistochemistry with the PA1-780 melanopsin antibody in a control (**A**, 181 days after vehicle injection) and a DM (**B**, 182 days after STZ injection) C57BL/6 mouse. Focal planes lie in the GCL. (**C, D**) Whole-retina mapping of immunostained cells shown in (**A**) and (**B**); each dot

represents a melanopsin-immunoreactive soma. D, dorsal; V, ventral; T, temporal; N, nasal. (**E**) No significant difference was detected in whole-retina melanopsin-positive cell number between control and DM retinas harvested at 180–195 days after DM induction. Sample sizes are given in parentheses. Scale bar = 100 μm in (**B**) and 1 mm in (**D**).

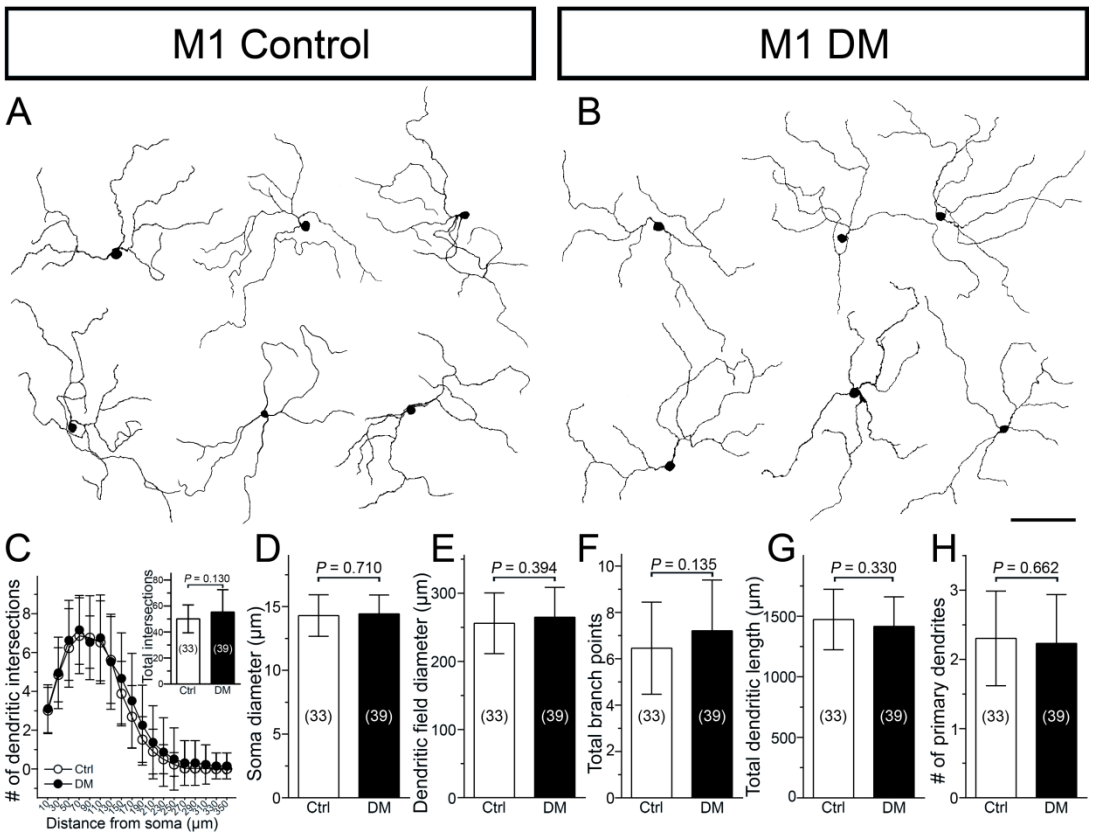

Supplementary Figure 6. 6-month diabetes did not change soma-dendritic profiles of M1 ipRGCs. (**A, B**) Representative examples of soma-dendritic profiles of M1 cells in control (**A**) and DM (**B**) mice, reconstructed from whole-mount retinas, which were harvested at 180–195 days after STZ administration. (**C**) Sholl analysis of M1 cells from control and 6-month DM mice revealed no significant changes in dendritic complexity. Inset is a bar graph comparing the total number of intersections between groups. (**D, E, F, G, H**) Bar graphs comparing major soma-dendritic parameters between control and 6-month DM mice. No significant difference was detected in any of these parameters. Sample sizes are given in parentheses. Scale bar = 100 μm.

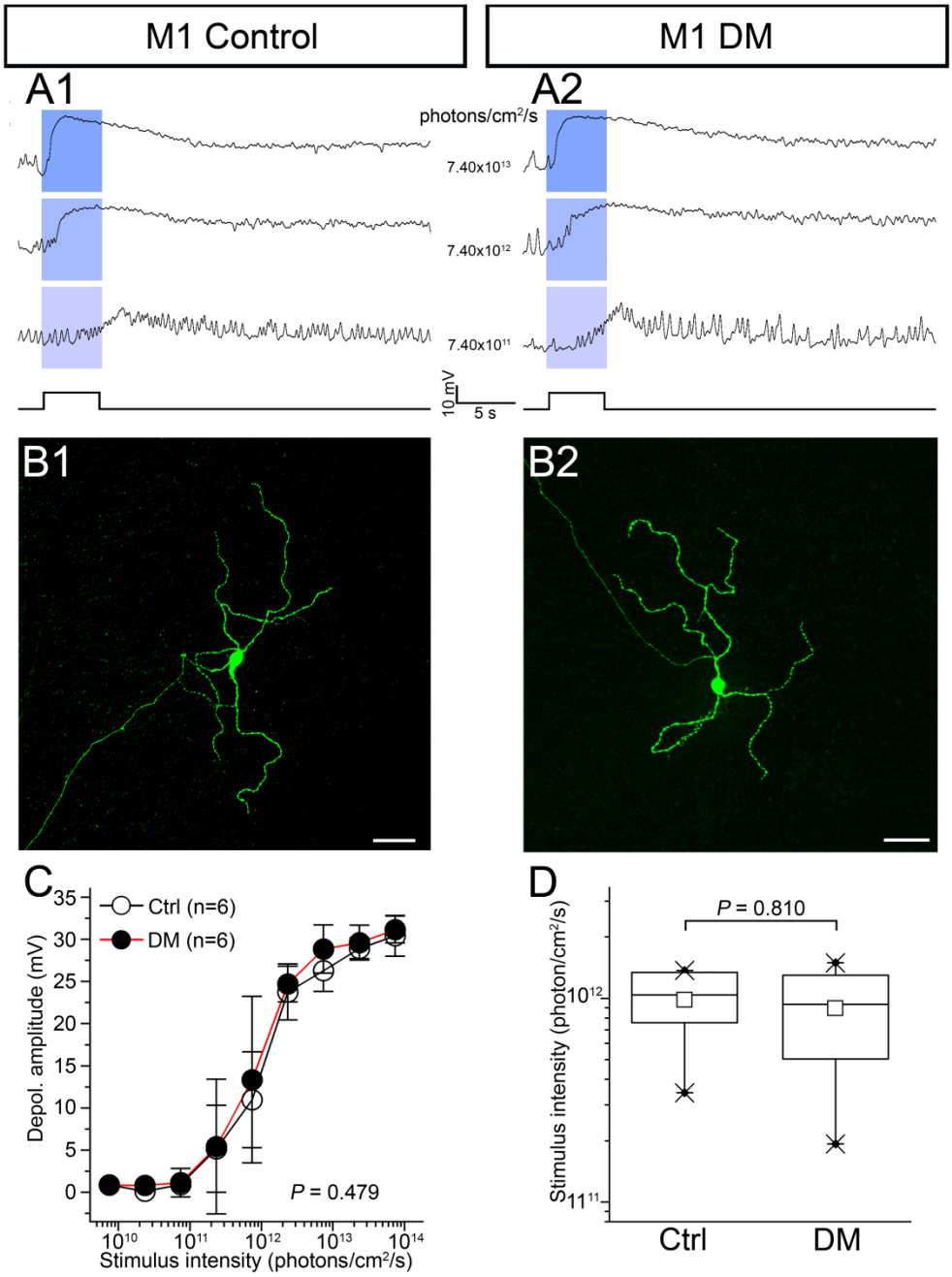

Supplementary Figure 7. Being hyperglycemic for 5–6 months did not significantly affect melanopsin-based photoresponses in M1 ipRGCs. (**A1, A2**) Representative melanopsin-based light responses of M1 cells to an intensity series of full-field, 480-nm light pulses, recorded in current-clamp mode in a control (**A1**, 157 days after vehicle injection) and a DM (**A2**, 166 days after STZ injection) *Opn4-tdTomato* retina in the presence of the glutamatergic cocktail. (**B1, B2**)

Confocal photomicrographs of whole-mount retinas showing the morphology of cells in (**A1**) and (**A2**) with typical dendritic branching characteristics revealed by neurobiotin included in the patch pipette. (**C**) Comparison of I–R curves, derived from peak depolarization amplitudes, revealed that the melanopsin-based photoresponse was unchanged in M1 cells collected from DM animals at 155–180 days after STZ treatment. (**D**) Pooled data demonstrating no significant difference in photoresponse threshold, calculated with Michaelis–Menten equation based on peak depolarization data, between control and DM M1 cells shown in (**C**). Scale bars = 50 μm. Sample sizes are given in parentheses.

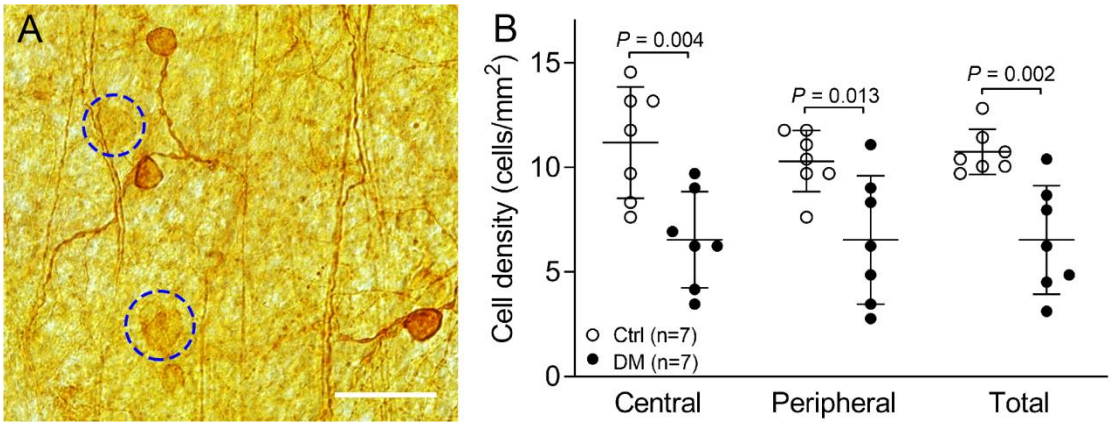

Supplementary Figure 8. Loss of M4-like cells in DM mice. (**A**) High magnification photomicrograph captured from whole-mount 3-month DM C57BL/6 retinas stained by enhanced immunohistochemistry with UF006 melanopsin antibody. Focal plane lies in the GCL. Dashed circles indicate two vaguely labeled "M4-like" cell bodies not visible under lower magnification, which are much larger than the neighboring intensely stained M1–M3 cells. (**B**) DM significantly reduced M4-like cell densities measured at central (694 × 520-μm regions centered at 0.6 mm from the optic nerve head), peripheral (694 × 520-μm regions centered at 1.5 mm from the optic nerve head) and entire (averages of central and peripheral regions) retina. Sample sizes are given in parentheses. Scale bar = 100 μm.

Animals

All data were obtained from C57BL/6 mice (male, Shanghai Laboratory Animal Center, Shanghai, China) or *Opn4-tdTomato* mice in a 129S;C57BL/6 mixed background (either sex), which were a generous gift from Dr. Tian Xue (University of Science and Technology of China, Hefei, Anhui, China). Animals were maintained in a temperature-controlled room (25 ± 1°C) under a 12-h light/12-h dark photoperiod (12L/12D), with food and water supplied *ad libitum*. All procedures were consistent with the ARVO Statement for the Use of Animals in Ophthalmic and Vision Research and were approved by the Institutional Animal Care and Use Committees of Fudan University.

Induction of experimental diabetes

Diabetes was chemically induced in mice aged 7–8 weeks with intraperitoneal injection of streptozotocin (STZ; 85 mg/kg body weight, Sigma-Aldrich Co., St. Louis, MO, USA) freshly dissolved in sodium citrate buffer (0.1 M, pH 4.5), for three consecutive days. Age-matched control mice received an equal volume of sodium citrate buffer. Blood glucose concentration and body weight were examined prior to injection and at 7 days, 1, 2, 3, 4, 5 and 6 months after the initial injection. Mice with fasting blood glucose levels exceeding 11.1 mM were considered to be diabetic (Supplementary Fig. 1).

Antibodies and biomarkers

The following primary antibodies and markers were used: polyclonal antibody raised in rabbits against the first 19 amino acid residues of the NH_2-terminal sequence of rat melanopsin (PA1-780; Fisher Scientific Inc., Barrington, IL, USA), which primarily labels M1 cells, but labels few, if any, non-M1 ipRGCs in mice (1-3); rabbit polyclonal antiserum probing a synthetic peptide consisting of the 15 NH_2-terminal amino acids of mouse melanopsin (UF006; Advanced Targeting Systems, San Diego, CA, USA), which clearly labels M1–M3 ipRGCs while faintly staining a few other ipRGCs in mice (4); goat polyclonal antibody recognizing Brn3a (Santa Cruz Biotechnology, Santa Cruz, CA, USA); and fluorescein-conjugated isolectin B4 (IB4) (Vector Laboratories, Burlingame, CA, USA), a marker for blood vessels. Secondary antibodies included biotinylated goat anti-rabbit IgG (Vector) for immunoperoxidase labeling and Alexa Fluor 488/555-conjugated donkey IgGs (Thermo Fisher Scientific, Waltham, MA, USA) for immunofluorescence.

Immunoperoxidase labeling

Animals were sacrificed by cervical dislocation. Eyes were removed immediately and placed in aerated Ames' medium (A1420, Sigma-Aldrich). The retina was subsequently dissected from the eyecup, mounted on a piece of filter paper (SCWP04700, Millipore, Billerica, MA, USA), and fixed for 2 h in 4% (w/v) paraformaldehyde (PFA) freshly prepared in phosphate-buffered saline (PBS; pH 7.4) at room temperature (RT). After washing with PBS (6 × 10 min), the retina was cryoprotected sequentially in 10%, 20% and 30% sucrose (2 h, RT). To further

enhance tissue permeability, the retina was freeze–thawed by briefly dipping it into liquid nitrogen, and then immersed in 0.5% dimethylsulfoxide (DMSO) and 2% Triton X-100 in Tris-buffered saline (TBS; pH7.4) at 4°C overnight. Endogenous peroxidase activity was quenched by immersion in 1% hydrogen peroxide in TBS (45 min, RT). After a blocking step (6% goat serum, 2% Triton X-100 and 0.5% DMSO in TBS, 2 h, RT), the retina flat mount was incubated in anti-melanopsin primary antibodies (UF006: 1:10000, 3 days; PA1-780: 1:1000, 7 days) at 4°C. The flat mount was again washed in TBS (6 × 10 min), and then incubated in biotinylated secondary antibody (1:200, 24 h, 4°C). The retina was transferred into an avidin–biotin–peroxidase complex (Elite ABC kit PK-6101, Vector) in TBS (2 h, RT), washed and pre-incubated under agitation in the dark with 3,3'-diaminobenzidine tetrahydrochloride (DAB, SK-4105, Vector; ice-bath, 5 min). After final washes in TBS (6 × 10 min), the retina was removed from the filter paper and mounted in glycerol onto a glass slide.

Fluorescent labeling

After fixation in PFA (2 h, RT), the whole-mount retina was washed in TBS (6 × 10 min) and blocked in a solution (5% goat serum and 1% Triton X-100 in TBS) for 2 h at RT, and incubated with primary antibodies (anti-Brn3a: 1:1000, 24 h; PA1-780: 1:1000, 7 days) in a buffer (1% bovine serum albumin, 3% goat serum and 1% Triton X-100 in TBS) at 4°C. After washing (6 × 10 min), secondary antibodies (1:400) were added and the tissue was incubated for 2 h at RT. After a final 6 × 10 min washes in

TBS, the free-floating retina was flat-mounted onto a glass slide and coverslipped. To label blood vessels, retinal whole mounts were incubated with fluorescein-conjugated IB4 (1:50, 24 h) with the same procedure as immunofluorescent labeling described above, but without any secondary antibody treatment.

Cell counting

Images of retinal whole mounts were taken by a fluorescence microscope (Axioskop 40, Carl Zeiss, Inc., Oberkochen, Germany). To count the total number of cells stained by melanopsin antibodies (PA1-780 or UF006), we collected a series of overlapping photomicrographs for each retina using a 10 × objective lens (N.A. 0.25). The entire retina was digitally reconstructed using Photoshop CS3 software (Adobe Systems, San Jose, CA, USA) and a silhouette showing the topographic distribution of melanopsin-positive cells was produced. These silhouettes were used to perform whole-retina cell counting. Cell bodies located in the GCL and those displaced to the INL were both counted. The density of Brn3a-positive conventional GCs and melanopsin (UF006)-positive M1–M3 ipRGCs, distinguished by dendritic stratification patterns in the IPL, were assessed under a 20 × objective lens (N.A. 0.8). Sample areas were eight 518 μm × 518 μm (for Brn3a) or 694 μm × 520 μm (for melanopsin) squares, regularly spaced along the horizontal and vertical meridians, four in the central and four in the peripheral retina (0.6 and 1.5 mm from the optic nerve head, respectively). Cells in each square were counted, and counts were pooled to calculate the mean cell density of the retina. The whole-retina area was delineated

using the Polygon tool in ImageJ software (NIH; http://imagej.nih.gov/ij/).

Morphometric analysis

Soma-dendritic profile reconstruction was conducted following the method developed by Berson el al. (4). Briefly, photomicrographs covering a small retinal area (typically ~900 μm × 500 μm) were collected at 1 μm intervals from multiple optical planes under a 40 × (N.A. 0.95) or 20 × (N.A. 0.8) objective lens. Melanopsin-positive somata and processes were in sharp focus in at least one image within such a stack of photomontages. Soma-dendritic profiles of individual ipRGCs in this retinal area were then traced using Photoshop CS3 software with the Pencil tool to create 2-D reconstructed drawings, which were transferred to ImageJ software for further processing and analysis. Soma diameter was calculated as the diameter of a circle, with area equal to the contour enclosing the cell body. Dendritic field diameter was estimated by calculating the diameter of a circle with area equal to that of a convex polygon minimally enclosing the dendritic field. Total dendritic length was measured using the NeuronJ plug-in of ImageJ (http://imagescience.org/meijering/software/neuronj/). Sholl analysis was performed using a plug-in developed in the Ghosh Laboratory at the Johns Hopkins University School of Medicine (http://ghoshlab.org/software/ShollAnalysis_.class).

Fluorescence intensity quantification of melanopsin-positive plexuses

Immunofluorescence images for intensity measurement were acquired using an

Olympus FV1000 confocal microscope (Olympus Corporation, Tokyo, Japan) under a 20 × objective lens (N.A. 0.75). The same acquisition settings were used for all image sets. For both ON and OFF melanopsin-positive plexuses, 1-μm-thick optical sections along the Z-axis were captured in a single retinal region and were processed with maximum intensity projection to create a composite. To minimize photobleaching, each region was imaged only once. Offline mean grey level measurement of the composite image was performed using Fiji software (http://imagej.net/Fiji) without any image enhancement. However, for clearer visualization, the overall brightness/contrast of representative images shown in Supplementary Figure 4 were slightly adjusted. The nonspecific background, measured by outlining areas in the outer part of the GCL where no melanopsin immunoreactivity was seen, was subtracted.

Western blotting

Western blot analysis was performed referring to a previous study (5). Briefly, freshly extracted retinal lysates (50 μg/lane) were electrophoresed by 12% sodium dodecyl sulfate polyacrylamide gel electrophoresis (SDS–PAGE) and electrophoretically transferred onto polyvinylidene fluoride (PVDF) membranes. Non-specific binding was blocked for 2 h at RT. Blots were then incubated with PA1-780 melanopsin antibody (1:500) overnight at 4°C, followed by horseradish peroxidase (HRP)-conjugated donkey anti-rabbit IgG (1:2000, Santa Cruz Biotechnology) for 2 h at RT. Immunoblots were visualized by enhanced chemiluminescence (Amersham

Biosciences, Piscataway, NJ, USA), and finally captured using the ChemiDoc XRS System with Image Lab software (Bio-Rad, Hercules, CA, USA).

Multi-electrode array (MEA) recording

Retina preparation

Procedures for MEA recording of melanopsin-based photoresponses have been described in detail previously (6; 7). The mouse was dark-adapted overnight (> 12 h) and then overdosed with 0.6% pentobarbital sodium. Under dim red light, one eye was immediately enucleated and transferred into Ames' medium equilibrated with 95% O_2 and 5% CO_2. The cornea was removed and the lens and vitreous extracted. The retina was dissected from the sclera, with a few very small radial cuts to help flattening, and then mounted, photoreceptor side down, on a piece of Anodisc filter membrane (Whatman, Piscataway, NJ, USA).

Data acquisition

The mounted retina was transferred into the recording chamber of an MEA chip (60MEA200/30iR-ITO-gr, MCS GmbH, Reutilingen, Genmany) and then continuously superfused at 5–6 mL/min with Ames' medium and maintained at 30 ± 2°C using a temperature controller (TC-324B, Warner Instruments, Hamden, CT, USA). Once in the chamber, the retina was kept light-tight, except when probed with test light pulses. Recording started after the retina had completely settled onto the array (usually ~45 min) with spike amplitudes stabilized. Voltage data were high-pass filtered at 200 Hz, digitized at 10 kHz, and amplified and acquired using the

USB-MEA60-Inv-BC-System and MC_Rack software (MCS).

Light stimulation

The retina was stimulated with a series of 10-s, 480-nm full-field light flashes at 3.42×10^{11} to 3.42×10^{14} photons/cm^2/s, generated by an LED illuminator (Model 66991, DiCon Fibersoptics Inc., Richmond, CA, USA) and delivered onto the retina by a fiber-optic cable. Light intensity was adjusted by introducing neutral density filters (Edmund Optics Inc., Barrington, NJ, USA) into the light path. Stimuli were presented in a series that was monotonically ascending in intensity and identical for all experiments. Inter-stimulus intervals increased progressively within the series, ranging from 5 min between dim stimuli to 10 min between the brightest stimuli.

Spike sorting and data analysis

Cluster analysis of the spikes was performed using a detection threshold of 3–4 times the standard deviation of the voltage with Offline Sorter software (Plexon Inc., Dallas, TX, USA). The resulting clusters were manually corrected for clustering errors. We derived four light response parameters from the spike data: 1) “spike number”, calculated by subtracting the number of spikes during the 10 s preceding light onset, from the sum of all action potentials occurring during light stimulus; 2) “peak firing rate”, calculated by subtracting the spontaneous resting firing rate during the 10 s preceding light stimulation, from the maximal firing rate during light stimulus; 3) “peak latency”, calculated as the time gap between stimulus onset and time of peak firing rate; and 4) “half decay time”, calculated as the time gap between the time of peak firing rate and the time when firing frequency decreased to half of the peak. The

I–R plot of the peak firing rate data of each cell was further fit by the Michaelis–Menten equation (6) to calculate the response threshold, which was the light intensity inducing 5% of the maximal light response.

Whole-cell patch clamp recording

The procedures of preparing whole mount of the *Opn4-tdTomato* retina were the same as those for MEA recording, except that the retina was mounted ganglion cell side up on a piece of Millipore filter paper (AABP02500) with a 2-mm-diameter hole to allow adequate infrared illumination and light stimulation. The whole mount was transferred into a recording chamber (RC-26GLP, Warner Instruments) and perfused (3–4 mL/min) with carbogen-saturated Ames' medium at 32–34°C. TdTomato-expressing cells were identified by epifluorescence evoked by a C-FL-C RFP filter set (Nikon Instruments Inc., Melville, NY, USA) and viewed using an upright microscope (FN-1, Nikon) equipped with a 40 × water immersion objective (N.A. 0.8) and a CMOS camera (optiMOS, QIMAGING, Surrey, Canada). To minimize photobleaching, the lowest excitation light intensity sufficient to reveal somatic tdTomato labeling was used; the total duration of epi-illumination did not exceed 5 s. After identification of a tdTomato-positive soma, current-clamp recordings were performed under visual control with infrared illumination. The patch pipette (tip resistance, 5–7 MΩ) contained (in mM): 120 K-methanesulfonate, 10 HEPES, 0.1 EGTA, 5 NaCl, 4 ATP-Mg, 0.4 GTP-Na_2, and 10 phosphocreatine-$Tris_2$, adjusted to pH7.2 and 280 mOsm. Signals were amplified using a MultiClamp 700B amplifier (Molecular

Devices, Sunnyvale, CA, USA), low-pass filtered at 2.4 kHz, and sampled at 10 kHz (Digidata 1550; Molecular Devices) in I = 0 mode. All reported voltages were corrected for a liquid junction potential of −10 mV. To measure the peak depolarization amplitude, raw recordings were offline low-pass filtered at 20 Hz to reduce the spike components of the signals and capture as many fast responses as possible. For clearer visualization, recording traces in Figure 7 and Supplementary Figure 7 were low-pass filtered with a 2-Hz cutoff. Full-field 5-s light stimuli were generated using a 100 W halogen lamp, band-pass filtered at 480 nm with a narrowband filter (Edmund), and presented from below the transparent bottom of the recording chamber. Light intensity was adjusted using neutral density filters (Edmund) and had intensities of 1.5×10^9 to 1.5×10^{15} photons/cm^2/s at the GCL. Each stimulus was followed by a dark recovery interval of 1–5 min, and then followed by the next stimulus. Stimulus timing was regulated using a logic-controlled electromechanical shutter (IQ35SA, Sutter Instrument Co., Novato, CA, USA).

Pupillometry

Before experiment, animals were dark-adapted for at least 12 hours. Measurements were restricted to the middle of the subjective day (ZT3–9). Under dim red illumination, the mouse was placed in a head-and-body restrainer device with a metal bar (implanted into the skull two days before the recording) fixed to the device and PLRs were recorded using a pupilometer (A2000; Neuroptics Inc., Irvine, CA, USA) in combination with Bandicam software (Bandicam Company, Seoul, South Korea).

The pupil of right eye was video monitored under infrared light with the left eye apposed to a series of light stimuli generated by a 463 nm LED, ranging from 2.33×10^7 photons/cm^2/s to 1.24×10^{15} photons/cm^2/s and presented in increasing order of intensity, following the initial baseline recording for 60 sec in dark. Each stimulus was presented for 60 sec, which was followed by 5 min of dark adaptation. Pupil area was then quantified manually in ImageJ software. The normalized pupil area was calculated as the pupil area after 30 sec of stimulus (steady state) relative to the dilated pupil size in dark. Data points were fitted with a sigmoidal dose-response curve to calculate EC_{50}.

Chemicals

To isolate melanopsin-based responses, the retina was bathed with a pharmacological cocktail [50 μM L-(+)-2-amino-4-phosphonobutyrate (L-AP4, group III metabotropic glutamate receptor agonist), 40 μM 6,7-dinitroquinoxaline-2,3-dione (DNQX, AMPA/kainate receptor antagonist), 2 μM (S)-1-(2-amino-2-carboxyethyl)-3-(2-carboxy-5-phenylthiophene-3-yl-methyl)-5-methylpyrimidine-2,4-dione (ACET, kainate receptor antagonist) and 30 μM D-2-amino-5-phosphonovalerate (D-AP5, NMDA receptor antagonist)], which blocks signaling from rods/cones to the inner retina. All pharmacological reagents were obtained from Tocris Biosciences (Ellisville, MO, USA) and were freshly prepared from aqueous stock solutions by dilution with Ames' medium.

Statistical analysis

Data are presented as mean ± SD when normally distributed and as median ± interquintile when non-normally distributed. Statistical analyses were performed using OriginPro 2015 software with unpaired *t*-test, two-sample Mann–Whitney *U* test, Kruskal-Wallis test and two-way ANOVA followed with appropriate *posthoc* multiple comparison tests. Unless otherwise specified, *P* values represented the results of unpaired *t*-test. A P value < 0.05 was considered as statistically significant.

Data and resource availability

The data generated in this study are available from the corresponding author upon request. No applicable resources were generated during this study.

References

1. van der Merwe I, Lukats A, Blahova V, Oosthuizen MK, Bennett NC, Nemec P: The topography of rods, cones and intrinsically photosensitive retinal ganglion cells in the retinas of a nocturnal (Micaelamys namaquensis) and a diurnal (Rhabdomys pumilio) rodent. *PLoS One* 13:e0202106, 2018

2. Wu XS, Wang YC, Liu TT, Wang L, Sun XH, Wang LQ, Weng SJ, Zhong YM: Morphological alterations of intrinsically photosensitive retinal ganglion cells after ablation of mouse photoreceptors with selective photocoagulation. *Exp Eye Res*:107812, 2019

3. Lin B, Peng EB: Retinal Ganglion Cells are Resistant to Photoreceptor Loss in Retinal Degeneration. *PLoS One* 8:e68084, 2013

4. Berson DM, Castrucci AM, Provencio I: Morphology and mosaics of melanopsin-expressing retinal ganglion cell types in mice. *J Comp Neurol* 518:2405-2422, 2010

5. Wu XH, Li YY, Zhang PP, Qian KW, Ding JH, Hu G, Weng SJ, Yang XL, Zhong YM: Unaltered retinal dopamine levels in a C57BL/6 mouse model of form-deprivation myopia. *Invest Ophthalmol Vis Sci* 56:967-977, 2015

6. Weng S, Estevez ME, Berson DM: Mouse ganglion-cell photoreceptors are driven by the most sensitive rod pathway and by both types of cones. *PLoS One* 8:e66480, 2013

7. Weng S, Wong KY, Berson DM: Circadian modulation of melanopsin-driven light response in rat ganglion-cell photoreceptors. *J Biol Rhythms* 24:391-402, 2009